Redox Biology 57 (2022) 102472

Contents lists available at ScienceDirect

Redox Biology

journal homepage: www.elsevier.com/locate/redox

Dietary intake of deuterium oxide decreases cochlear metabolism and oxidative stress levels in a mouse model of age-related hearing loss

Shule Hou [a,b,c,1], Penghui Chen [a,b,c,1,**], Jingchun He [a,b,c,1], Junmin Chen [a,b,c], Jifang Zhang [a,b,c], Fabio Mammano [d,e,***], Jun Yang [a,b,c,*]

[a] Department of Otorhinolaryngology-Head & Neck Surgery, Xinhua Hospital, Shanghai Jiaotong University School of Medicine, Shanghai, China
[b] Shanghai Jiaotong University School of Medicine Ear Institute, Shanghai, China
[c] Shanghai Key Laboratory of Translational Medicine on Ear and Nose Diseases, Shanghai, China
[d] Department of Physics and Astronomy "G. Galilei", University of Padua, Padova, Italy
[e] Department of Biomedical Sciences, Institute of Cell Biology and Neurobiology, Italian National Research Council, Monterotondo, Italy

ARTICLE INFO

Keywords:
Deuterium oxide
Age related hearing loss
Cochlea
Metabolism
Oxidative stress

ABSTRACT

Age-related hearing loss (ARHL) is the most prevalent sensory disorder in the elderly. Currently, no treatment can effectively prevent or reverse ARHL. Aging auditory organs are often accompanied by exacerbated oxidative stress and metabolic deterioration. Here, we report the effect of deuterated oxygen (D_2O), also known as "heavy water", mouse models of ARHL. Supplementing the normal mouse diet with 10% D_2O from 4 to 9 weeks of age lowered hearing thresholds at selected frequencies in treated mice compared to untreated control group. Oxidative stress levels were significantly reduced and in the cochlear duct of treated vs. untreated mice. Through metabolic flux analysis, we found that D_2O mainly slowed down catabolic reactions, and may delay metabolic deterioration related to aging to a certain extent. Experiments confirmed that the Nrf2/HO-1/glutathione axis was down-regulated in treated mice. Thus, D_2O supplementation can hinder ARHL progression in mouse models by slowing the pace of metabolism and reducing endogenous oxidative stress production in the cochlea. These findings open new avenues for protecting the cochlea from oxidative stress and regulating metabolism to prevent ARHL.

Introduction

With the population aging, the incidence rate of ARHL, the third most common chronic disease in the elderly [1], has been gradually increasing [2]. Patients with ARHL develop insidious, progressive, and slow bilateral high-frequency hearing loss, which affects speech recognition and sound source localization, increases risk of Alzheimer's disease and reduces the quality of life [2–4]. In addition, ARHL causes a series of adverse effects on psychology, physiology and society [5–7].

ARHL is accompanied by imbalance of reactive oxygen species (ROS) and progressive deterioration of metabolism in the inner ear [8]. ROS, as a group of metabolic products including superoxide, hydroxyl radicals, and hydrogen peroxide, can peroxidase membrane lipids of cells and organelles, and damage both DNA and proteins [9]. Deregulated ROS production has been clearly associated with ARHL in both humans and mice [10,11]. The latter are widely used as a model for ARHL research [12–14]. Other pathways may also serve as important targets to delay aging and are implicated in hearing protection in mouse models. For example, treatment with the mTORC1 inhibitor rapamycin prevents Tsc/mTORC1–dependent hearing impairment [15]. Genetic deletion of mTORC1 in the cochlear neurosensory epithelium also protects mice against ARHL [15]. In addition, caloric restriction (CR) and long-term regular exercise slowed the progression of ARHL by reducing oxidative stress or inflammation in mice [16,17]. However, treatment options

* Corresponding author. Department of Otorhinolaryngology-Head & Neck Surgery, Xinhua Hospital, Shanghai Jiaotong University School of Medicine, Shanghai, China.
** Corresponding author. Department of Otorhinolaryngology-Head & Neck Surgery, Xinhua Hospital, Shanghai Jiaotong University School of Medicine, Shanghai, China.
*** Corresponding author. Department of Physics and Astronomy "G. Galilei", University of Padua, Padova, Italy.
E-mail addresses: cph_shsmu@163.com (P. Chen), fabio.mammano@unipd.it (F. Mammano), yangjun@xinhuamed.com.cn (J. Yang).
[1] These authors contributed equally to this work.

https://doi.org/10.1016/j.redox.2022.102472
Received 15 June 2022; Received in revised form 6 September 2022; Accepted 8 September 2022
Available online 17 September 2022

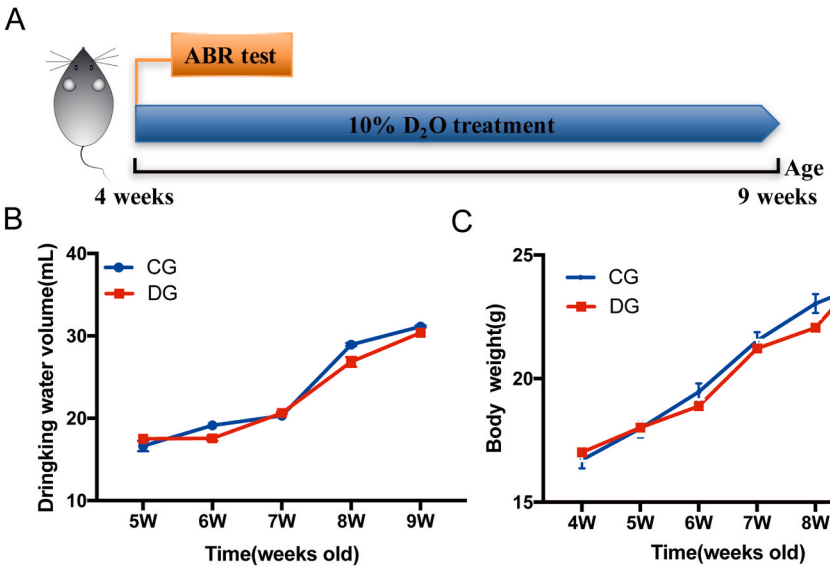

Fig. 1. Experimental procedure and measurement of drinking water volume and body weight. **A**) Scheme of D_2O administration. **B, C**) Time course of mouse drinking water volume (B) and body weight (C) of D_2O-treated group (DG) and control group (CG). Data are shown as mean ± SEM; $n = 18$ mice for each group. The ABR test was repeated at 9, 20 and 40 weeks of age (not shown).

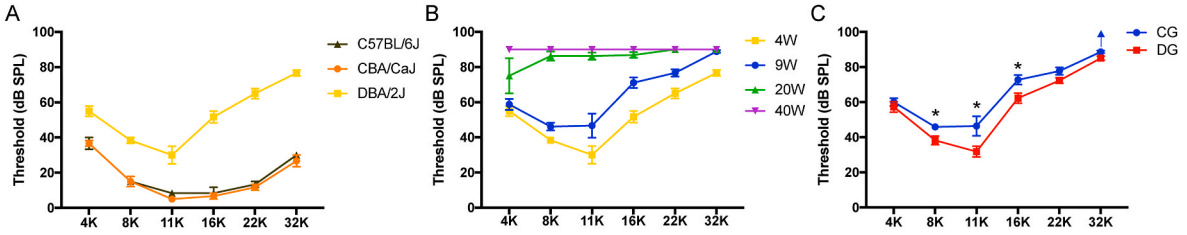

Fig. 2. Effect of dietary D_2O supplementation on auditory thresholds of DBA/2J mice. **A)** Auditory threshold evaluation by i*n vivo* auditory brainstem recordings (ABRs) at 4 weeks of age in C57BL/6J, CBA/Caj, DBA/2J mice (n = 3 mice per group). Data (mean ± SEM) were computed from tone burst responses at 4, 8, 11, 16, 22 and 32 kHz. **B)** Auditory threshold evaluation by ABRs at 4, 9, 20 and 40 weeks of age in DBA/2J mice (n = 3 mice in 4W group, n = 8 mice in other groups). **C)** Auditory thresholds at 9 weeks in DBA/2J mice (DG, D_2O administration group; CG, control group; n = 8 mice per group). P-values were determined by two-tailed *t*-test. *, P<0.05, **, P<0.01.

to effectively prevent or reverse ARHL in clinical use are basically non-existent [18]. Preventing ARHL through environmental intervention or nutrient uptake is an interesting approach that is worth exploring, even though the underlying mechanisms are incompletely understood.

D_2O has a molecular weight of 20.0275 Da, which is about 11% higher than that of H_2O [19]. Since the late 1950s, deuterium isotopes have been used in investigational drugs for the treatment of pancreatic cancer, hypertension, respiratory viral diseases, and skin herpesvirus diseases [20–22]. D_2O was reported to inhibit ROS production in yeast and rodents [23,24]. In addition, yeast longevity experiment showed that heavy isotopes modulated metabolism, suppressed endogenous generation of ROS, and lead to better long-term sustainability and longevity [25]. Therefore, we hypothesized that D_2O might protect rodents from ARHL by modifying metabolism in the inner ear.

To test our hypothesis, we examined the effect of dietary D_2O supplementation on the progression of ARHL in DBA/2J mice. With mutations in cadherin 23 (CDH23) and fascin-2 (fscn2), DBA/2J mice develop early-onset progressive hearing loss that is already detectable at one month of age, and are widely used as model for ARHL research [26–28]. We tested hearing performance in these mice by auditory brainstem response (ABR) recordings [29] and correlated the results to metabolic flux analyses [30]. For comparison, we also examined C57BL/6J and CBA/CaJ mice, the two most widely used inbred strains in hearing research [31,32]. C57BL/6J mice exhibit a high frequency hearing loss by 3–6 months of age that progresses to a profound impairment by 15 months due to the mutation of CDH23 [33–35]. The CBA/CaJ strain does not have this predisposing CDH23 variant, remains resistant to ARHL until 15 months of age or older, and are often used as good hearing controls [36]. We found that D_2O supplementation can slow the pace of metabolism and reduce endogenous oxidative stress in the cochlea, as shown by a reduced activation of the Nrf2/HO-1/glutathione axis that plays a pivotal role in oxidative stress regulation [37].

Materials and Methods

Animals and treatment

DBA/2J and CBA/CaJ mice were purchased from Shanghai SIPPR-BK Laboratory Animals Co. Ltd. C57BL/6J mice were purchased from Shanghai Slac Laboratory Animals Co. Ltd. All animal experimentation was performed in accordance with the guidelines approved by the experimental animal care institution of Xinhua Hospital, Medical College of Shanghai Jiaotong University. Mice were housed in the group on a schedule of 12 h of light and 12 h of darkness, and they had free access to food and water. We inspected the ears of the mice, and those with infections in the external auditory canal and middle ear were excluded. Mice that received 5 weeks of treatment with 10% D_2O from postnatal week 4 to week 9 will be referred to as D_2O treatment group (DG), whereas age-matched untreated mice will be referred to as control group

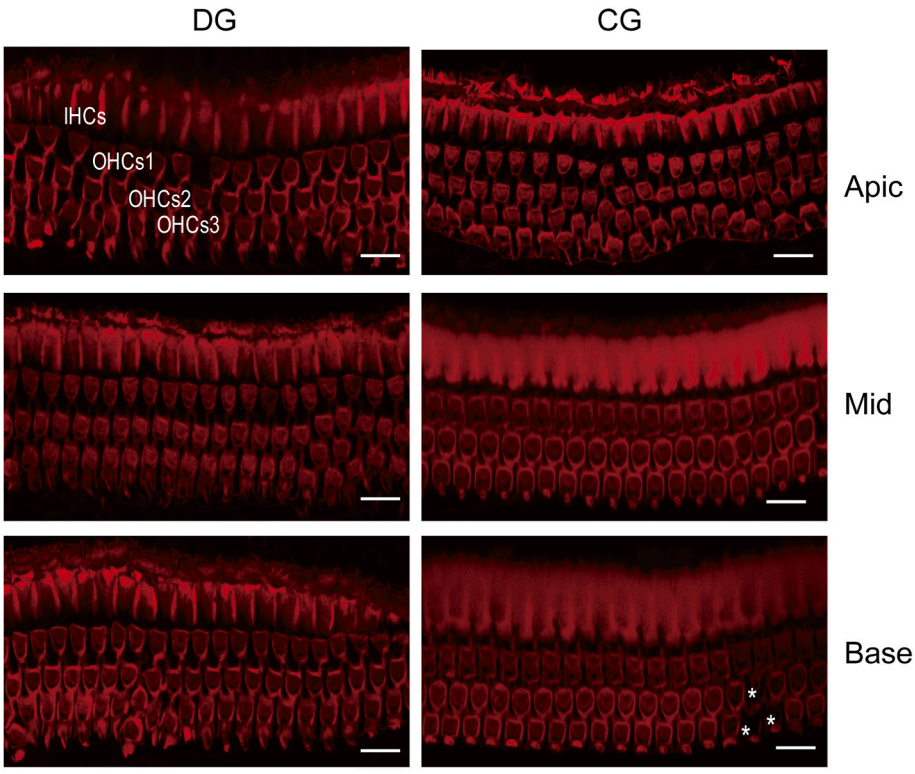

Fig. 3. Effect of dietary D_2O supplementation on hair cell survival in DBA/2J mice. Shown are whole-mounts of the cochlea sensory epithelium from mice at 9 weeks. DG, D_2O administration group; CG, control group. Inner hair cells (IHCs) and outer hair cells (OHCs) were stained with phalloidin-Alexa 594 (red), and images from apical (Apic), middle (Mid) and basal (Base) turns were obtained by laser scanning confocal microscopy; * indicate missing hair cells; scale bar:100 μm. For data quantification, see Table 1. (For interpretation of the references to colour in this figure legend, the reader is referred to the Web version of this article.)

Table 1
of hair cell survival in the apical, middle and basal turn of the mouse cochlea at 9 weeks of age. DG, D_2O administration group; CG, control group (n = 3 mice per group). Shown are mean percent values, rounded to nearest integer, with standard deviation (in round brackets) and p-values (in square brackets) of DG samples relative to CG controls as determined by the Mann-Whitney *U* test.

Organ of Corti	inner hair cells survival (%)		outer hair cells survival (%)	
	DG	CG	DG	CG
Apical Turn	100(0)	99(1) p=0.058	99(1)	98(1) [p=0.289]
Middle Turn	100(0)	100(0) p=1.00	100(1)	99(1) [p=0.296]
Basel Turn	99(1)	98(1) p=0.758	98(1)	96(2) [p=0.012]

(CG) (Fig. 1A). One-hundred and twenty (120) male mice of each strain were randomly divided into D_2O DG and CG, 60 in each group-. CG mice received sterilized drinking water, whereas DG mice received 10% heavy water (#151882, Sigma-Aldrich, USA). Both fluids were offered daily in normal drinking bottles over a 5-weeks period.

Measurement of ABRs

Mice were anesthetized with intraperitoneal injections of ketamine (70 mg/g) and medetomidine (1 mg/g). The depth of anesthesia was periodically verified by the lack of foot pinch response. Body temperature was maintained at 37 °C using a heating pad. For ABR recordings, acoustic stimuli consisted of tone bursts of 4, 8, 11,16, 22, and 32 kHz, which were delivered in the free field using an MF1-M speaker. ABRs were recorded using sub-dermal needle electrodes with gauge 27, 13

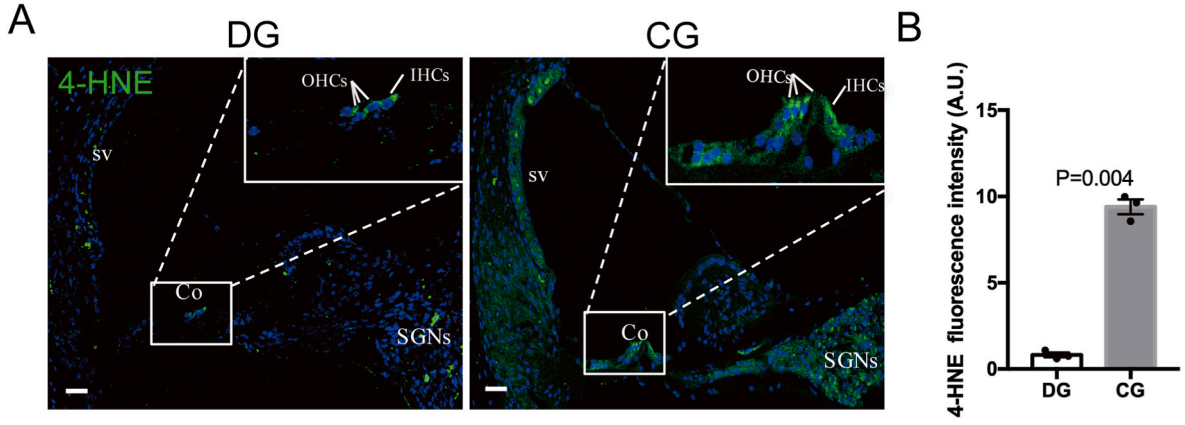

Fig. 4. Effect of dietary D_2O supplementation on lipid peroxidation in the cochlea of DBA/2J mice. **A**) Representative confocal images of anti-4-HNE immunofluorescence staining and DAPI fluorescence-in mid-modiolar transversal cryosections of DG and CG samples at 9 weeks of age. Scale bars: 50 μm. SV, *stria vascularis*; CO, Corti's organ; SGNs, spiral ganglion neurons; IHCs, inner hair cells; OHCs, outer hair cells. **B**) Histograms of fluorescence emission intensity values for anti-4-HNE; A.U., arbitrary units; Experiments were performed in triplicate and p-values (P) were determined by two-tailed *t*-test.

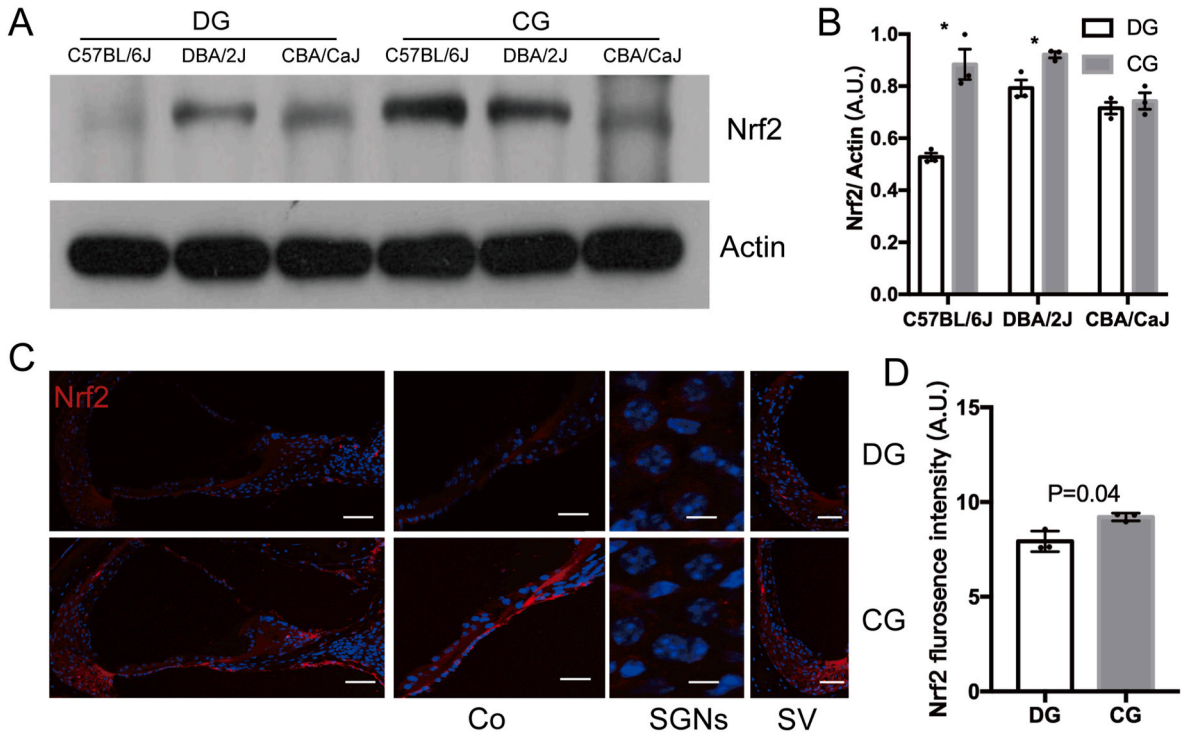

Fig. 5. Effect of dietary D_2O supplementation on Nrf2 expression in the cochlea of DBA/2J, C57BL/6J and CBA/CaJ mice. **A**) Western blot analysis of Nrf2 expression in the cochlea of mice at 9 weeks of age; DG, D_2O administration group; CG, control group. **B**) Histograms (mean ± SEM) of blot optical density values normalized to actin. **C**) Immunofluorescence analysis of Nrf2 (red fluorescence) in the organ of Corti (Co), spiral ganglion neurons (SGNs) and stria vascularis (SV) at 9 weeks of age in DBA/2J mice. Scale bars: 200 μm; Co, 20 μm; SGNs, 15 μm; StV, 50 μm. **D**) Histograms (mean ± SEM) of fluorescence intensity values for Nrf2. Experiments were performed in triplicate, and p-values (P) in (B) and (D) were determined by two-tailed *t*-test. *, $P<0.05$. (For interpretation of the references to colour in this figure legend, the reader is referred to the Web version of this article.)

mm needle electrodes (#S83018-R9, Rochester) inserted at the vertex (Active), ventrolateral to the left ear (Reference) and hind hip (Ground). Potentials were amplified, filtered (0.3–3 kHz), and averaged over 512 identical stimuli. Hearing threshold levels were determined offline as the sound pressure level (SPL) for which a Wave II peak could be visually identified above the noise floor (0.1 μV) at the specified frequencies.

Immunofluorescence staining and confocal imaging

After the final ABR test, animals (n=6) were anesthetized (ketamine, 70 mg/g) and sacrificed by cervical dislocation. Both cochleae were quickly removed and fixed with 4% paraformaldehyde (PFA, #G1101, Servicebio, China), pH 7.5, at 4 °C overnight. Cochleae were then decalcified for 3 days in 10% ethylene diamine tetraacetic acid (EDTA, #G1105, Servicebio, China) at room temperature, dehydrated by 15% sucrose solution for 2 days and 30% sucrose solution for additional 2 days, and embedded in Opti-mum Cutting Temperature Compound (OCT, #4583S, SAKURA, USA). Then, the tissue was cut into 8 μm sections using a histology cryostat (Leica, CM1950, Germany).

Specimens were first incubated with a blocking solution (0.5% Triton X-100 (#T8787, Sigma-Aldrich, USA) and 10% normal donkey serum (#S26-M, Sigma-Aldrich, USA) in 0.1 M PBS, and then with a solution containing anti-nuclear factor erythroid 2-related factor 2 (Nrf2, #ab89443, Abcam, USA), anti-Heme-oxygenase 1 (HO-1, #ADI- SPA-896D Stressgen, Canada) or anti-glutathione (GSH, #ab19534, Abcam, USA) primary antibodies diluted 1:100 in 0.01 M PBS overnight at 4 °C. The anti-GSH antibody was generated using GSH conjugated to Keyhole limpet hemocyanin (KLH) as immunogen. The antibody reacts with GSH-protein complexes under non-reducing conditions. KLH is a large, multi-subunit, oxygen-carrying, metalloprotein found in certain aquatic snails; it is used extensively as a carrier protein in the production of antibodies for research, biotechnology and therapeutic applications, see e.g. Ref. [38]. After washing in 0.01 M PBS for 15 min three times, samples were incubated in fluorescently labeled secondary antibodies: goat anti-rabbit (HO-1) (Alexa Fluor 488 # A-11034, ThermoFischer Scientific) or donkey anti-mouse (GSH, Nrf2) (Alexa Fluor 594, #ab150108, Abcam, USA) diluted 1:500 in 0.01 M PBS at room temperature for 2 h. Nuclei were counterstained with 4′,6-diamidino-2-phenylindole (DAPI).

To quantify hair cell survival, cochlear sensory epithelia were quickly dissected and fixed with 4% PFA for 2 h. Thereafter, tissues were stained with TRITC Phalloidin (#T4104780, YEASEN, China) for 30 min at room temperature.

All samples were mounted onto glass slides with an anti-fade medium (#ZG1028, VECTOR) and analyzed using a confocal microscope (SP5, Leica, Germany) equipped with air (20x) and oil–immersion (40x) objectives (Leica).

Detection of lipid peroxidation

Reactive oxygen species generation and elimination in living things are in a state of dynamic equilibrium. Biological macromolecules, including lipid peroxidation, can be harmed when this balance is upset by a variety of reasons and the concentration of reactive oxygen species exceeds physiological limits. For lipid peroxidation, dissected cochleae were incubated with a blocking solution (1% BSA, 0.5% Triton X-100 and 10% normal goat serum in PBS 0.1 M), and then with a solution containing a polyclonal a primary antibody selective for 4-hydroxy-2-nonenal (4-HNE), (#HNE11-S, Alpha Diagnostic Int., USA; this antibody was obtained from rabbits immunized against 4-HNE conjugated to KLH) diluted 1:100 in PBS overnight at 4 °C. Thereafter, specimens were incubated with a fluorescently labeled goat anti-rabbit secondary antibody (Alexa Fluor 488, #A32731, ThermoFisher , USA) diluted 1:400 in 0.01 M PBS at room temperature for 2 h. Finally, samples were

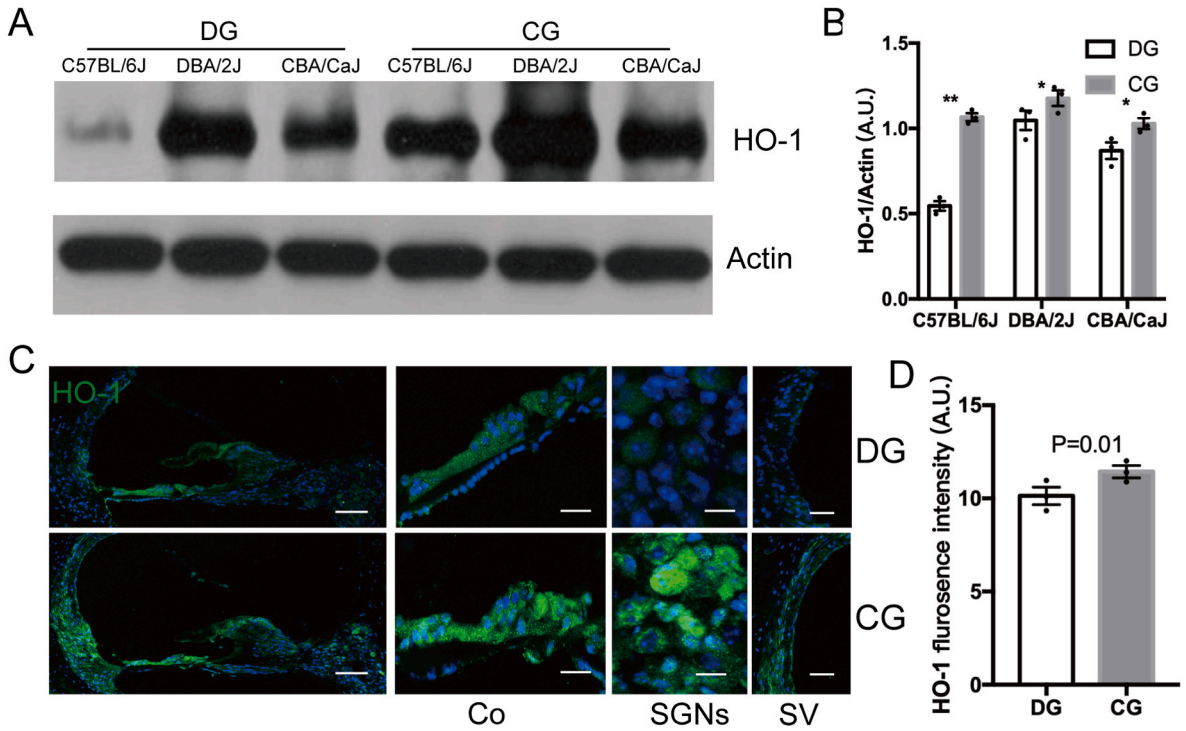

Fig. 6. Effect of dietary D_2O supplementation on HO-1 expression in the cochlea of DBA/2J, C57BL/6J and CBA/CaJ mice. **A**) Western blot analysis of HO-1 expression in the cochlea of mice at 9 weeks of age; DG, D_2O administration group; CG, control group. **B**) Histograms (mean ± SEM) of blot optical density values normalized to actin. **C**) Immunofluorescence analysis of HO-1 expression (green fluorescence) in the organ of Corti (Co), spiral ganglion neurons (SGNs) and stria vascularis (SV) at 9 weeks of age in DBA/2J DG and CG mice. Scale bars: 200 μm; Co, 20 μm; SGNs, 15 μm; StV, 50 μm. **D**) Histograms (mean ± SEM) of fluorescence intensity values for HO-1. Experiments were performed in triplicate, and p-values (P) in (B) and (D) were determined by two-tailed *t*-test. *, $P<0.05$; **, $P<0.01$. (For interpretation of the references to colour in this figure legend, the reader is referred to the Web version of this article.)

counter-stained with DAPI (1:1000 in 0.01 M PBS).

Western blotting analyses

Nine-weeks old C57BL/6J, DBA/2J and CBA/Caj mice (n=10 animals of each strain) were anesthetized (ketamine, 70 mg/g), sacrificed by cervical dislocation, and both cochleae were quickly removed. Samples used for GSH analyses were processed under non reducing conditions to identify multiple bands at variable molecular weights to detect all glutathionylated proteins. Proteins were isolated by SDS-PAGE on 10% polyacrylamide gels and transferred to polyvinylidene fluoride (PVDF) membranes (Millipore, USA). The membranes were blocked (Beyotime, China) at ambient temperature for 1 h and probed with the following primary antibodies at 4 °C for overnight: anti-Nrf2 (1:1000; # ab89443, Abcam, USA); anti HO-1 (1:1000; #ADI-SPA-896D, StressGen Biotechnology, Canada); anti-GSH (1:1000; #19534, Abcam, USA), and anti-actin (1:2000; #60004, Proteintech, USA). After three washes in 0.01 M PBS, the membranes were incubated with a secondary antibody, either HRP-labeled Goat anti-rabbit IgG, or anti-mouse IgG (1:1000; Beyotime, A0208/A0216, China), at 37 °C for 1 h. Subsequently, the chemiluminescence reagent (Millipore, A: B=1:1, USA) was utilized to develop the immunoreactive bands, and images were analyzed using the Bio-Rad ChemiDoc XRS+ (Bio-Rad Company, USA). At least three independent experiments were carried out. Fiji-Image J (NIH) software to measure the intensities of the bands. The band densities were normalized to background. Values were expressed as Nrf2 and HO-1/actin ratio. For GSH quantification, values were expressed as optical density of multiple bands at all molecular weights.

Metabolic flux analysis

Eight nine-weeks old DBA/2J mice from DG or CG (n=2 animals each sample, which are recorded as D1, D2, D3, D4 and C1, C2, C3, C4 respectively) were anesthetized (ketamine, 70 mg/g), sacrificed by cervical dislocation, and both cochleae were quickly removed. The fibrous tissue and blood on the surface of cochlear bony capsule were gently removed using 0.9%NaCl solution. Each sample included four cochleae (about 50 mg). For each 50 mg sample, we added 1250 μL of cold extraction solvent (methanol: acetonitrile: water = 2:2:1, v/v/v). The sample was homogenized twice using a homogenizer (FastPrep-24, MP, Biomedicals, USA) with the following parameters: 24 × 2 ml tubes of size, 6.0 m/s of power, 60 s of time. The homogenate was sonicated twice at low temperature (30 min each round), then the mixture was centrifuged for 5 min (14000 g, 4 °C) and the supernatant was thoroughly lyophilized (FreeZone 6 L, Labconco, USA) in a vacuum centrifuge.

Prior to measurement, the samples were re-dissolved in 50 μL of methanol/water (1:1, v/v) solvent. Mass spectrometry (MS) measurements of isotopic distribution were performed by Shanghai Applied Protein Technology Co., Ltd. using an ultrahigh performance liquid chromatography apparatus (Vanquish UHPLC, ThermoFisger Scientif) coupled to a Orbitrap (Q Exactive HF-X) For Hydrophilic interaction liquid chromatography (HILIC) separation, samples were analyzed using a SeQuant ZIC-HILIC column (100 mm × 2.1 mm i.d., 3.5 μm) (Merck, Germany). In both electron spray ionization (ESI) positive and negative modes, the mobile phase contained A=50 mM ammonium formate in water and B=acetonitrile. The gradient was 0–10 min (90–50% B), 10–12 min (50–90% B), 12–15 min (90% B). The gradients were run at a flow rate of 0.4 mL/min, and column temperatures were kept constant at 45 °C. 1 μL aliquot of each sample was injected into the sampler of the UHPLC instrument. MS data were acquired in full scan mode: mass range, *m/z* 100 to 1000; scan time, 0.2s. Retention times and mass estimates for each compound were confirmed against calibration standards as well as matched unlabeled cochlea extracts under the same

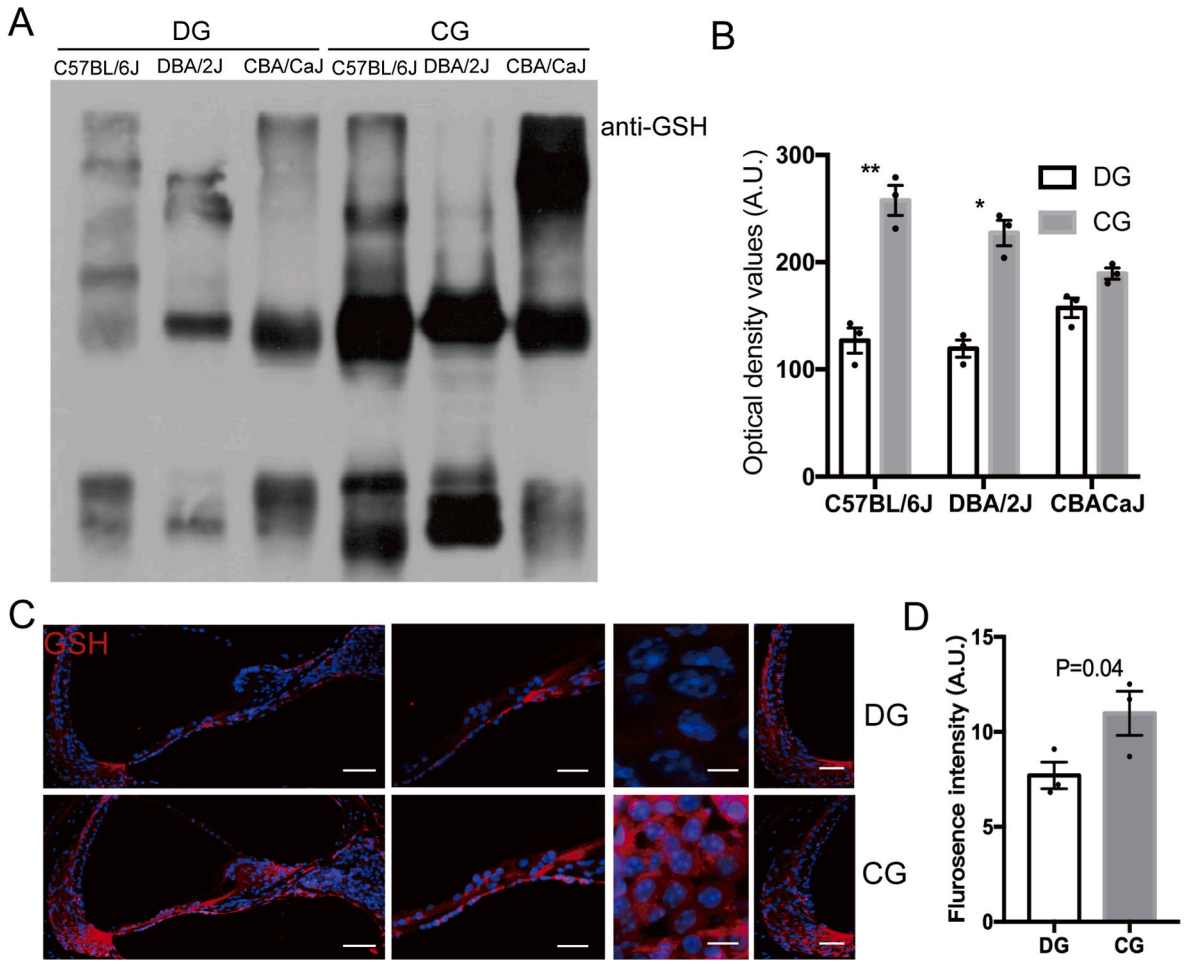

Fig. 7. Effect of dietary D_2O supplementation on glutathionylated protein expression in the cochlea of DBA/2J, C57BL/6J and CBA/CaJ mice. **A**) Western blot analysis of glutathionylated protein expression in DG and CG cochleae at 9 weeks of age. **B**) Histograms (mean ± SEM) of blot optical density values normalized to actin. **C**) Immunofluorescence analysis of glutathionylated protein (red fluorescence) in the organ of Corti (Co), spiral ganglion neurons (SGNs) and stria vascularis (SV) at 9 weeks of DBA/2J mice. Scale bars: 200 μm; Co, 20 μm; SGNs, 15 μm; StV, 50 μm. **D**) Histograms (mean ± SEM) of fluorescence intensity values for glutathionylated protein. Experiments were performed in triplicate and p-values (P) in (B) and (D) were determined by two-tailed *t*-test. *, P<0.05; **, P<0.01. (For interpretation of the references to colour in this figure legend, the reader is referred to the Web version of this article.)

conditions.

Correction for natural abundance of isotope is required prior to meaningful interpretation. The correction used both a generally applicable correction matrix, based on Eqn. (1), and an isotopic correction matrix that was generated by treating a control group of unlabeled samples. Data processing and ion annotation based on mass estimate were performed in TraceFinder 5.0 (ThermoFisher Scientific) and Xcalibur 4.0 (ThermoFisher Scientific).

$$\begin{pmatrix} I_0 \\ I_1 \\ I_2 \\ \cdots \\ I_n \\ \cdots \\ I_{n+u} \end{pmatrix} = \begin{pmatrix} L_0^{M_0} & 0 & 0 & \cdots & 0 \\ L_1^{M_0} & L_0^{M_1} & 0 & \cdots & 0 \\ L_2^{M_0} & L_1^{M_1} & L_0^{M_2} & \cdots & 0 \\ \cdots & \cdots & \cdots & \cdots & \cdots \\ L_n^{M_0} & L_{n-1}^{M_1} & L_{n-2}^{M_2} & \cdots & \cdots \\ \cdots & \cdots & \cdots & \cdots & \cdots \\ L_{n+u}^{M_0} & L_{n+u-1}^{M_1} & L_{n+u-2}^{M_2} & \cdots & L_u^{M_n} \end{pmatrix} \cdot \begin{pmatrix} M_0 \\ M_1 \\ M_2 \\ \cdots \\ M_n \end{pmatrix} \quad (1)$$

I, the fractional abundances of the measured metabolite ions.

M, the MDV corrected for naturally occurring isotopes,

n, the number of carbon atoms that are present in the analyzed metabolite ion,

u, additional measured ion abundances beyond n originating from natural isotopes in the metabolite.

L, the correction matrix.

Statistical analysis

Data are presented as mean ± standard error of the mean (SEM) and were analyzed using the GraphPad Prism 8.0 software. All data were obtained in at least n=3 independent experiments. Statistical analysis was conducted by Student's two-tailed *t*-test (Microsoft Office Excel 2016); $P < 0.05$ indicate statistical significance.

Results

Dietary D_2O supplementation ameliorates ARHL in DBA/2J mice and protects cochlear hair cells

For these experiments, we performed dietary D_2O supplementation as described in the Materials and Methods (Fig. 1A). Mice that received 5 weeks of treatment with 10% D_2O from postnatal week 4 to week 9 will be referred to as D_2O treatment group (DG), whereas age-matched untreated mice will be referred to as control group (CG). We also measured mouse drinking water volume and mouse body weight to determine the effect of daily D_2O administration on body mass. DG mice presented no significant difference of drinking water volume and body weight compared to CG mice (Fig. 1B, **C**).

To establish a baseline for the hearing performance of each of the three mouse strains used in this study (DBA/2J, C57BL/6J and CBA/

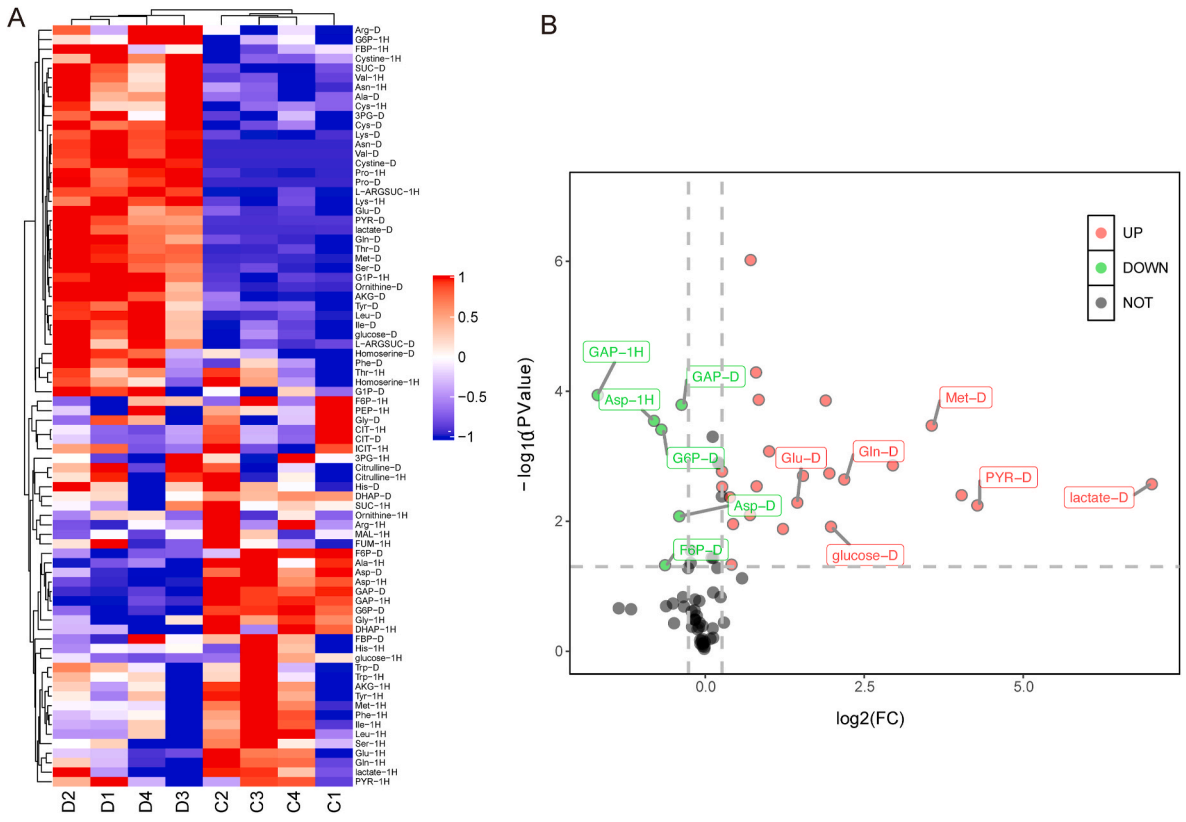

Fig. 8. Effect of dietary D_2O supplementation on metabolite levels in the cochlea of DBA/2J mice. **A**) Heat map of metabolites differentially expressed in the cochlea; D1-D4: samples from D_2O administration group (DG); C1–C4: samples from control group (CG); n = 4 mice per group. **B**) Volcano plot analysis showing protein expressed with different abundance in the cochlea of DG and CG mice. 1H: 1H isotope only, D: Sum of D isotopes.

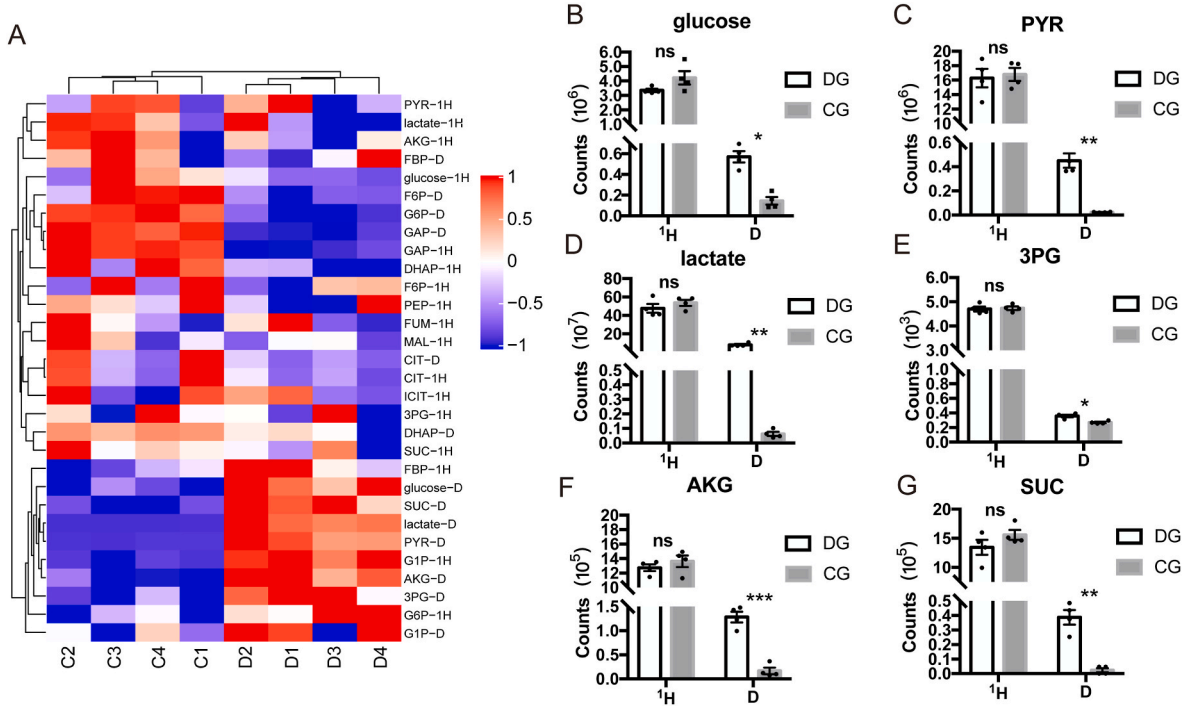

Fig. 9. Effect of dietary D_2O supplementation on glucose metabolism and tricarboxylic acid cycle (TCA) in the cochlea of DBA/2J mice. **A**) Heat map of metabolites differentially expressed in the cochlea. D1-D4: samples from D_2O administration group (DG); C1–C4: samples from control group (CG); n = 4 mice per group. **B-G**) Histograms showing different abundance of metabolite expression in the cochlea of DG and CG mice. 3 PG: 3-Phosphoglyceric acid, PYR: Pyruvate, AKG: 2-Oxoglutarate, SUC: Succinate. P-values (P) were determined by two-tailed *t*-test. *, P<0.05; **, P<0.01; ***, P<0.001. ^{1}H: ^{1}H isotope only, D: Sum of D isotopes.

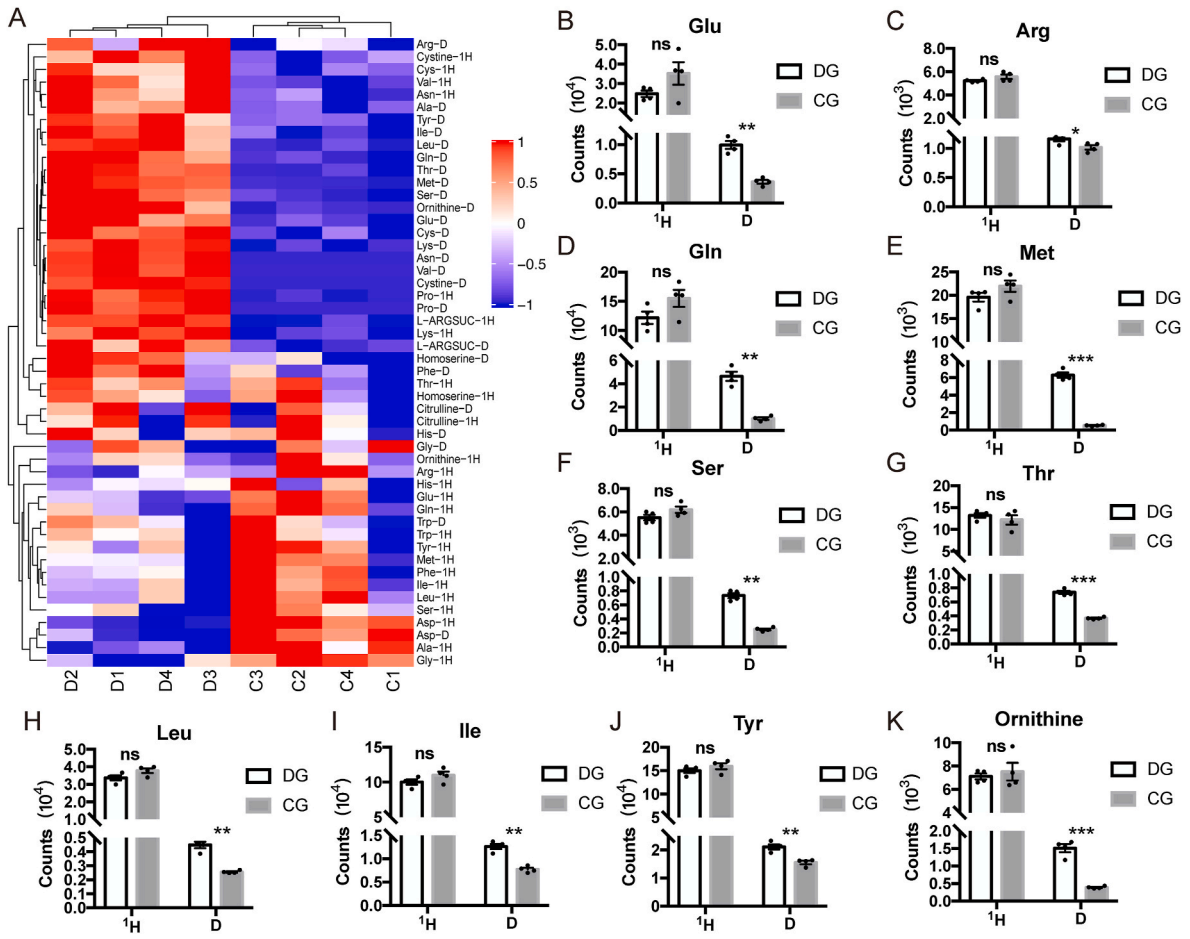

Fig. 10. Effect of dietary D_2O supplementation on amino acid metabolism in the cochlea of DBA/2J mice. **A**) Heat map of metabolites differentially expressed in the cochlea. D1-D4: samples from D_2O administration group (DG); C1–C4: samples from control group (CG); n = 4 mice per group. (B–K) Histograms showing the different abundance of metabolite expression in the cochlea of DG and CG mice. Glu: Glutamic acid, Gln: Glutamine, Leu: Leucine, Ile: Isoleucine, Arg: Arginine, Ser: Serine, Thr: Threonine, Tyr: Tyrosine, Met: Methionine. P-values (P) were determined by two-tailed *t*-test. *, P<0.05; **, P<0.01; ***, P<0.001. ^{1}H: ^{1}H isotope only, D: Sum of D isotopes.

CaJ), we estimated hearing thresholds (HTs) by analyzing ABRs to pure tone stimuli at 4 weeks, 9 weeks, 20 weeks, and 40 weeks of age in a frequency range comprised between 4 and 32 kHz. As previously reported [26,39], DBA/2J mice exhibited an early onset (4 weeks), progressive, high-frequency (>16 kHz) hearing loss (Fig. 2A). At 9 weeks, HTs of DBA/2J mice were significantly elevated compared to 4 weeks' HTs, with a minimum of about 50 dB SPL at 11 kHz, reaching 60- and 90-dB SPL at the lower and upper end of the spectrum, respectively. At 20 weeks, HTs exceed 80 dB SPL at all frequencies above 8 kHz. At 40 weeks, haring loss of DBA/2J mice at this age was severe, with HTs in exceeding 90 dB SPL at all frequencies (Fig. 2B). HTs of DBA/2J DG mice, measured at 9 weeks of age, were significantly lower at 8, 11 and 16 kHz than HTs of their respective frequency in CG mice (Fig. 2C). These findings correlate with a significant difference between the percentage of outer hair cell (OHC) survival in the sensory epithelium of basal cochlear turns in DG vs. CG mice (Fig. 3 and Table 1).

Dietary D_2O supplementation decreases endogenous oxidative stress in the cochlea

As mentioned in the Introduction, there is compelling evidence for a correlation between ARHL and oxidative stress in both humans and mice [10,11]. In prior work, 4-HNE assays were used to probe, lipid peroxidation in fixed samples of the rodent cochlea [40,41].

4-HNE is a well-known highly reactive by-product of lipid peroxidation that is widely accepted as a stable marker for oxidative stress and may contribute to the cytotoxic effects of oxidative stress [42]. 4-HNE can react with several functional groups on biological material, particularly sulfydryl groups to form thioester adduct and then hemiacetals. 4-HNE may also react with histidine and lysine residues of proteins to form stable Michael addition-type of adducts. Antibodies to 4-HNE can help to visualize the HNE-adducts [43].

Here, to determine whether dietary D_2O supplementation affected oxidative stress levels in the cochlea, we performed confocal fluorescence imaging of fixed cochlear sections immunolabelled with an anti-4-HNE antibody (see Materials and Methods). The fluorescence emission of 4-HNE immunoreactivity (Fig. 4A and B) in the *stria vascularis* (SV), spiral ganglion neurons (SGNs) and Corti's organ (Co) were significantly lower in DBA/2J DG mice compared to their CG, suggesting D_2O supplementation reduced ROS production and/or potentiated the response of the endogenous antioxidant defense system.

The nuclear factor erythroid 2-related factor 2 (NRF2) is a transcription factor (encoded by the *Nrf2* gene) that is activated in response to oxidative stress [44]. The activated NRF2 proteins translocate to the nucleus, where they induce the expression of numerous antioxidant response element (ARE) genes, including the gene that encodes heme oxygenase-1 (HO-1) [45]. The NRF2/ARE/HO-1 axis has a protective role in noise-induced oxidative damage of cochlea [40]. Therefore, we also examined the effects of dietary D_2O supplementation on the expression levels of NRF2 and HO-1 proteins by western blots (Fig. 5A and B and Fig. 6A and B) and immunofluorescence with antibodies selective for NRF2 (Fig. 5C and D) and HO-1 (Fig. 6C and D). At 9 weeks of

age, expression levels of both proteins were significantly reduced in DG compared to CG mice, and the decrease was also evident in SGNs, Co, and SV of DBA/2J mice (Figs. 5 and 6).

Protection from oxidative damage may involve upregulation of glutathione (GSH), a small peptide composed of three amino acids (cysteine, glutamic acid, and glycine) [46]. GSH is an important antioxidant whose levels depend on the concerted activity of glutathione synthetase (GS), glutathione reductase (GR), glutathione peroxidase (GPX) and glutathione-S-transferase (GST) [46], and the genes encoding these enzymes are all under control of the NRF2/ARE pathway [37]. The Western blot results in Fig. 7A, **B** show a decrease of glutathionylated protein at different molecular weights under non-reducing conditions in DG mice at 9 weeks of age. Immunofluorescence image analysis, presented in Fig. 7C and D, confirmed that glutathionylated protein levels (red fluorescence) decreased in SGNs, Co, and SV in DGs compared to their respective CG in DBA/2J mice.

Together, these results suggest that dietary D_2O supplementation diminished endogenous ROS levels, thereby reducing the need for NRF2-dependent protection mechanisms.

Dietary D_2O supplementation mainly slowed down catabolic reactions and may delay the metabolic deterioration related to aging

Given that heavy isotopes modulated metabolism of yeast [25], we asked whether dietary D_2O supplementation might counteract metabolic deterioration associated with ARHL in mice. To this end, we compared metabolism of different substrates, including 25 amino acids and key intermediate products involved in glycolysis and tricarboxylic acid cycle by metabolic flux analysis in the inner ear. To assess the effect of deuterium incorporation on the metabolome, we also compared two forms of metabolites: one for only 1H isotopic forms, and the other using the sum of all D-isotopic forms of each metabolite (Figs. 8–10). Heat map and Volcano plot analysis in Fig. 8 showed all metabolites differentially expressed in the cochlea between in DG and in CG. Volcano plot analysis in Fig. 8B showed most of up-regulated metabolites in DG than in CG are with D-isotope.

The metabolism of amino acids includes 1) synthesis of proteins, peptides, and other nitrogen-containing substances; 2) decomposition into α-ketoacids, amines and carbon dioxide. α-ketoacids can be converted into sugars, lipids or some non-essential amino acids, or be oxidized into carbon dioxide and water through the tricarboxylic acid cycle coupled to energy release. The essential amino acids are those 8 that cannot be synthesized and are required by the body, including Leu, Lys, Met, Phe, Ile, Trp, Thr and Val. Ten out of 25 amino acids (Leu, Ile, Thr, Tyr, Gln, Glu, Arg, Ser, Met, and ornithine) showed no difference in 1H and increased in D on DG vs CG (Fig. 9). Five amino acids (Phe, His, Trp, citrulline, homoserine) were not affected, showing no difference in both 1H and D. Eight amino acids (Lys, Cys, Pro, L-Argsuc, cytine, Val, Asn, and Gly) showed both 1H and D increase in DG mice. Only Asp showed 1H and D decrease in DG mice. Ala showed 1H decrease and D increase in DG mice. In brief, 19 out of 25 amino acids showed D increase in DG mice.

Glucose metabolism can be divided into catabolism and anabolism. The catabolism of glucose mainly includes anaerobic glycolysis and aerobic oxidation. Anaerobic glycolysis produces various metabolites and releases less energy. Aerobic oxidation produces carbon dioxide and water, and release more of energy. The tricarboxylic acid cycle is the common metabolic pathway of the three nutrients (carbohydrates, lipids, and amino acids), and it is also the hub of carbohydrate, lipid and amino acid metabolism. Eighteen kinds of key intermediate products involving glycolysis and tricarboxylic acid cycle were detected in our experiments (Fig. 10): glucose, lactate, 3 PG, SUC, PYR, and AKC showed that 1H was unchanged, and D was increased in DG mice; F6P and DHAP showed 1H remained unchanged and D decreased in DG mice.

The overall metabolites with 1H form displayed only slight changes, while most of deuterate labeled metabolites were accumulated more in DG than in CG mice (Fig. 8B, the data we used is DG vs CG, and the fold change value and P value obtained are reported), indicating that D_2O dietary supplementation did not distort the entire metabolome and did suppress catabolism of deuterated metabolites. Together, metabolic flux analysis showed D_2O mainly slowed down catabolic reactions involving glucose and amino acids, and thus may delay metabolic deterioration related to aging, to a certain extent.

Dietary D_2O supplementation also ameliorates ARHL in C57BL/6J and CBA/CaJ mouse models and decreases endogenous oxidative stress in the cochlea

Given the great differences in hearing threshold and hearing loss among ARHL individuals [2], studying potential hearing-protective effect in different mouse strains with different hearing loss progression might increase the translatable value of candidate drugs. Therefore, we used two other ARHL mouse models (C57BL/6J mice and CBA/CaJ mice) to examine the effect of D_2O on ARHL progression. We administered 10% D_2O dietary supplementation starting at 4 weeks of age, and performed ABR tests at 9 weeks of age. We found significantly lower HTs at 32 kHz in C57BL/6J mice, and at 4 kHz in CBA/CaJ mice, respectively (Fig. S1). There was no difference of the percentage of inner hair cell (IHC) and OHC survival in the sensory epithelium between in DG vs. CG mice (Fig. S2 and Table S1).

In the cochleae of C57BL/6J and CBA/CaJ mice, 4-HNE, used as endogenous ROS markers, were clearly reduced in the cochlea of DG mice compared to control mice (Fig. S3). On the other hand, immunoblotting and immunofluorescence data showed that the expression of Nrf2, HO-1, and glutathione in DG cochleae were all decreased compared to CG cochleae (Fig. S4). The Nrf2/HO-1 pathway and glutathione metabolism pathway were also inhibited in DG cochlea (Figs. 5–7).

These results suggest that D_2O might ameliorate different types of ARHL.

Discussion

ARHL is a complex disease with multiple factors [1,47], whose underlying mechanisms remain unclear. Here, we report D_2O dietary supplementation ameliorates ARHL in the DBA/2J mouse model of ARHL. D_2O suppressed endogenous oxidative stress production and reduced activation of the Nrf2/HO-1/glutathione axis. Metabolic flux analysis showed that D_2O decelerated the consumption of nutrients such as glucose and amino acids, mainly slowed down the catabolic reaction, and may delay metabolic deterioration related to aging to a certain extent. Thus, D_2O supplementation can reduce ARHL progression in mouse models by slowing the pace of metabolism and reducing endogenous oxidative stress production in the inner ear.

As mentioned in the Introduction, the redox environment of the inner ear is intimately connected with the aging process [11]. Antioxidant uptake can slow down ARHL progression in experimental models, and the efficacy of some antioxidants was confirmed in clinical studies [48–50]. When endogenous ROS increase with aging, antioxidant genes are up-regulated to constitute a defense against ROS and establish a detoxification system to maintain ROS balance. Heavy isotopes have been proposed to potentially confer chemical resistance to ROS [23,24]. Differently from the effects of other antioxidants, the reduced expression of the antioxidant genes in this study showed that D_2O dietary supplementation may bypass the Nrf2/HO-1/glutathione axis, directly suppressing internal ROS generation in the cochlea, and eventually reduce hearing impairment in ARHL mice. Therefore, D_2O likely acts on common upstream, downstream, or in parallel to these genetic regulations in protecting from hearing loss [25].

In three mouse models with different deafness mechanism and genetic background, D_2O conferred resistance to ARHL by decreasing

oxidative stress production without exception, which also supports the above speculation. Similarly, CR works as an effective environmental intervention to reduces ROS, extend lifespan, and protect from ARHL in different models through different intracellular pathways [51–53]. Thus, both D_2O uptake and CR are effective environmental intervention for hearing protection against aging. However, it is unknown whether D_2O suppresses oxidative stress production by reducing free radical damages to intracellular targets, or by decreasing oxidative phosphorylation, a major source of intracellular ROS, or both [54].

Most of deuterate labeled metabolites accumulated more in DG than in CG mice, suggesting that D_2O dietary supplementation may slow down catabolic reactions. There are significant kinetic differences, because the increase of charge weight increases the stability of chemical bonds containing heavy isotopes (for example, D-C is 5–10 times more stable than H–C).Thus, heavy isotopes may greatly reduce the reactivity of chemical bonds, making them less vulnerable to chemical damage [22], a phenomenon known as kinetic isotope effect (KIE). In addition, D_2O can increase the stability of proteins and other molecules by strengthening the formation of hydrophobic bonds [55]. Therefore, D_2O reduces the rate of all hydrolysis reactions, which are mostly catabolic. Energy mainly comes from catabolism, hence decreased catabolism may lead to reduced energy availability. Similarly, CR protects against ARHL and extends the life span [16,52,53]. Consistent with the findings, we inferred that D_2O may mimic the effects of CR by retarding age-related metabolic deterioration, inhibiting oxidative stress production and slowing down ARHL by KIE. Compared with CG, nineteen out of 25 amino acids (Leu, Ile, Thr, Tyr, Gln, Glu, Arg, Ser, Met, ornithine, Lys, Cys, Pro, L-Argsuc, cytine, Val, Asn, Gly and Ala) showed increased in D of DG, including three branched chain amino acids (BCCA: Leu, Ile, Val). Several studies have concluded that BCAA have a positive effect on aging by activating mTOR [56–59]· Gln has universality and importance in metabolism [60,61]. Gln reduction with age is caused by changes in several metabolic activities, including energy production (such as oxidative phosphorylation) and waste disposal (such as catabolic amino acid metabolism) [25]. Gln in D was considerably higher in the DG group than in the CG group, and the reduction of Gln with aging was eased, suggesting that D_2O may be one of the effectors in delaying aging. Compared to CG, the upstream glycolytic intermediates GAP were lower in DG. However, the downstream glycolytic intermediates 3 PG and PYR as well as various TCA cycle intermediates like AKG and SUC were all significantly elevated. Glycolysis appears to be localized to the region between GAP and PYR in light of these findings. Taken together, these considerations suggest that controlling metabolism deterioration in aging is an ideal therapeutic modality for ARHL.

It remains unknown whether dietary D_2O supplementation causes metabolic blockade and developmental delay or reduced survival. D_2O can hinder the growth and metabolism of many multicellular organisms, but it extends the longevity of yeast or the fertility of fruit flies [25,62]. However, no mouse mortality and adverse event occurred in this study, and there was no significant difference in body weight between experimental and control mice. Previous studies have shown that moderate body deuteration has few side effects and that both mice and rats tolerated D_2O well [63–65]. Therefore, it may be one of the goals of future work to determine the best dosage and duration of D_2O intake. One limitation of our study is that the actual D-label in vivo has not been determined. In other studies, D_2O enrichment was estimated by nuclear magnetic resonance (NMR) [66] of blood samples. We hope that follow-up studies will provide a solid and reliable basis for the clinical translation of D_2O-based treatment of ARHL.

Conclusion

In this study, we showed that dietary D_2O supplementation can slow the pace of metabolism and reduce endogenous oxidative stress production in the cochlea, bypassing the Nrf2/HO-1/glutathione axis. Importantly, we concluded that D_2O supplementation modified oxidative stress levels in the inner ear, and showed protective effects against ARHL in different mouse models. Adjusting metabolic flows appears to be a possible target to delay hearing loss due to aging.

Declaration of competing interest

The authors declare that the research was conducted in the absence of any commercial or financial relationships that could be construed as a potential conflict of interest.

Data availability

Data will be made available on request.

Acknowledgement

This work is supported by grants from National Science Foundation of China (82000977 to SL, 82230035, 82271179, 81873698 to JY, 82000989 to PC), and Shanghai Sailing Program (20YF1428900 to SL, 20YF1428800 to PC). We thank Mr. Caihua Zhu from Shanghai Applied Protein Technology for his technical support.

Appendix A. Supplementary data

Supplementary data to this article can be found online at https://doi.org/10.1016/j.redox.2022.102472.

Abbreviations

ARHL	age-related hearing loss
SGNs	spiral ganglion neurons
ROS	reactive oxygen species
SPL	sound pressure level
PFA	paraformaldehyde
EDTA	ethylene diamine tetraacetic acid
ABRs	auditory brainstem responses
SEM	standard error of the mean
HTs	hearing thresholds
Co	Corti's organ
SV	stria vascularis
4-HNE	4-hydroxy-2-nonenal
Nrf2	nuclear factor erythroid 2
ARE	antioxidant response element
HO-1	heme oxygenase-1
GSH	glutathione
GS	glutathione synthetase
GR	glutathione reductase
GPX	glutathione peroxidase
GST	glutathione-S-transferase
3 PG	3-Phosphoglyceric acid
PYR	Pyruvate
AKG	2-Oxoglutarate
SUC	Succinate
Glu	Glutamic acid
Gln	Glutamine
Leu	Leucine
Ile	Isoleucine
Arg	Arginine
Ser	Serine
Thr	Threonine
Tyr	Tyrosine
Met	Methionine

References

[1] M.R. Bowl, S.J. Dawson, Age-related hearing loss, Cold Spring Harb Perspect Med 9 (8) (2019), https://doi.org/10.1101/cshperspect.a033217.

[2] Y. Agrawal, E.A. Platz, J.K. Niparko, Prevalence of hearing loss and differences by demographic characteristics among US adults: data from the National Health and Nutrition Examination Survey, 1999-2004, Arch. Intern. Med. 168 (14) (2008) 1522–1530, https://doi.org/10.1001/archinte.168.14.1522.

[3] K. Slade, C.J. Plack, H.E. Nuttall, The effects of age-related hearing loss on the brain and cognitive function, Trends Neurosci. 43 (10) (2020) 810–821, https://doi.org/10.1016/j.tins.2020.07.005.

[4] J.S. Golub, A.M. Brickman, A.J. Ciarleglio, N. Schupf, J.A. Luchsinger, Association of subclinical hearing loss with cognitive performance, JAMA Otolaryngol Head Neck Surg 146 (1) (2020) 57–67, https://doi.org/10.1001/jamaoto.2019.3375.

[5] R. Patel, B.J. McKinnon, Hearing loss in the elderly, Clin. Geriatr. Med. 34 (2) (2018) 163–174, https://doi.org/10.1016/j.cger.2018.01.001.

[6] Y. Uchida, S. Sugiura, Y. Nishita, N. Saji, M. Sone, H. Ueda, Age-related hearing loss and cognitive decline - the potential mechanisms linking the two, Auris Nasus Larynx 46 (1) (2019) 1–9, https://doi.org/10.1016/j.anl.2018.08.010.

[7] S. Cosh, C. Helmer, C. Delcourt, T.G. Robins, P.J. Tully, Depression in elderly patients with hearing loss: current perspectives, Clin. Interv. Aging 14 (2019) 1471–1480, https://doi.org/10.2147/CIA.S195824.

[8] C. López-Otín, M.A. Blasco, L. Partridge, M. Serrano, G. Kroemer, The hallmarks of aging, Cell 153 (6) (2013) 1194–1217, https://doi.org/10.1016/j.cell.2013.05.039.

[9] B. Yang, Y. Chen, J. Shi, Reactive oxygen species (ROS)-Based nanomedicine, Chem. Rev. 119 (8) (2019) 4881–4985, https://doi.org/10.1021/acs.chemrev.8b00626.

[10] J. Chester, E. Johnston, D. Walker, et al., A review on recent advancement on age-related hearing loss: the applications of nanotechnology, drug pharmacology, and biotechnology, Pharmaceutics 13 (7) (2021), https://doi.org/10.3390/pharmaceutics13071041.

[11] J. Menardo, Y. Tang, S. Ladrech, et al., Oxidative stress, inflammation, and autophagic stress as the key mechanisms of premature age-related hearing loss in SAMP8 mouse Cochlea, Antioxidants Redox Signal. 16 (3) (2012) 263–274, https://doi.org/10.1089/ars.2011.4037.

[12] S.N. Park, S.A. Back, K.H. Park, et al., Comparison of cochlear morphology and apoptosis in mouse models of presbycusis, Clin Exp Otorhinolaryngol 3 (3) (2010) 126–135, https://doi.org/10.3342/ceo.2010.3.3.126.

[13] S.G. Kujawa, M.C. Liberman, Translating animal models to human therapeutics in noise-induced and age-related hearing loss, Hear. Res. 377 (2019) 44–52, https://doi.org/10.1016/j.heares.2019.03.003.

[14] K.K. Ohlemiller, S.M. Jones, K.R. Johnson, Application of mouse models to research in hearing and balance, J Assoc Res Otolaryngol 17 (6) (2016) 493–523, https://doi.org/10.1007/s10162-016-0589-1.

[15] X. Fu, X. Sun, L. Zhang, et al., Tuberous sclerosis complex-mediated mTORC1 overactivation promotes age-related hearing loss, J. Clin. Invest. 128 (11) (2018) 4938–4955, https://doi.org/10.1172/JCI98058.

[16] S. Someya, W. Yu, W.C. Hallows, et al., Sirt3 mediates reduction of oxidative damage and prevention of age-related hearing loss under caloric restriction, Cell 143 (5) (2010) 802–812, https://doi.org/10.1016/j.cell.2010.10.002.

[17] C. Han, D. Ding, M.C. Lopez, et al., Effects of long-term exercise on age-related hearing loss in mice, J. Neurosci. 36 (44) (2016) 11308–11319, https://doi.org/10.1523/JNEUROSCI.2493-16.2016.

[18] J. Wang, J.L. Puel, Presbycusis: an update on cochlear mechanisms and therapies, J. Clin. Med. 9 (1) (2020), https://doi.org/10.3390/jcm9010218.

[19] G.N. Lewis, The biology of heavy water, Science 79 (2042) (1934) 151–153, https://doi.org/10.1126/science.79.2042.151.

[20] W.C. Bila, A.E. Freitas, A.S. Galdino, E. Ferriolli, K. Pfrimer, J.A. Lamounier, Deuterium oxide dilution and body composition in overweight and obese schoolchildren aged 6-9 years, J. Pediatr. 92 (1) (2016) 46–52, https://doi.org/10.1016/j.jped.2015.03.007.

[21] A.M. Huges, B.M. Tolbert, K. Lonberf-Holm, M. Calvin, The effect of deuterium oxide on survival of mice with ascites tumor, Biochim. Biophys. Acta 28 (1) (1958) 58–61, https://doi.org/10.1016/0006-3002(58)90427-x.

[22] D.J. Kushner, A. Baker, T.G. Dunstall, Pharmacological uses and perspectives of heavy water and deuterated compounds, Can. J. Physiol. Pharmacol. 77 (2) (1999) 79–88, https://doi.org/10.1139/y99-005.

[23] I.A. Pomytkin, O.E. Kolesova, Relationship between natural concentration of heavy water isotopologs and rate of H2O2 generation by mitochondria, Bull. Exp. Biol. Med. 142 (5) (2006) 570–572, https://doi.org/10.1007/s10517-006-0420-9.

[24] M.S. Shchepinov, Reactive oxygen species, isotope effect, essential nutrients, and enhanced longevity, Rejuvenation Res. 10 (1) (2007) 47–59, https://doi.org/10.1089/rej.2006.0506.

[25] X. Li, M.P. Snyder, Yeast longevity promoted by reversing aging-associated decline in heavy isotope content, NPJ Aging Mech Dis 2 (2016), 16004, https://doi.org/10.1038/npjamd.2016.4.

[26] T. Kondo, S. Saigo, S. Ugawa, et al., Prebiotic effect of fructo-oligosaccharides on the inner ear of DBA/2 J mice with early-onset progressive hearing loss, J. Nutr. Biochem. 75 (2020), 108247, https://doi.org/10.1016/j.jnutbio.2019.108247.

[27] K.R. Johnson, C. Longo-Guess, L.H. Gagnon, H. Yu, Q.Y. Zheng, A locus on distal chromosome 11 (ahl8) and its interaction with Cdh23 ahl underlie the early onset, age-related hearing loss of DBA/2J mice, Genomics 92 (4) (2008) 219–225, https://doi.org/10.1016/j.ygeno.2008.06.007.

[28] X. Liu, M. Zhao, Y. Xie, et al., Null mutation of the Fascin2 gene by TALEN leading to progressive hearing loss and retinal degeneration in C57bl/6J mice, G3 (Bethesda) 8 (10) (2018) 3221–3230, https://doi.org/10.1534/g3.118.200405.

[29] Q.Y. Zheng, K.R. Johnson, L.C. Erway, Assessment of hearing in 80 inbred strains of mice by ABR threshold analyses, Hear. Res. 130 (1–2) (1999) 94–107, https://doi.org/10.1016/s0378-5955(99)00003-9.

[30] S.B. Crown, M.R. Antoniewicz, Parallel labeling experiments and metabolic flux analysis: past, present and future methodologies, Metab. Eng. 16 (2013) 21–32, https://doi.org/10.1016/j.ymben.2012.11.010.

[31] K.L. Kane, C.M. Longo-Guess, L.H. Gagnon, D. Ding, R.J. Salvi, K.R. Johnson, Genetic background effects on age-related hearing loss associated with Cdh23 variants in mice, Hear. Res. 283 (1–2) (2012) 80–88, https://doi.org/10.1016/j.heares.2011.11.007.

[32] H.S. Li, E. Borg, Age-related loss of auditory sensitivity in two mouse genotypes, Acta Otolaryngol. 111 (5) (1991) 827–834, https://doi.org/10.3109/00016489109138418.

[33] A.L. Burghard, N.P. Morel, D.L. Oliver, Mice heterozygous for the Cdh23/Ahl1 mutation show age-related deficits in auditory temporal processing, Neurobiol. Aging 81 (2019) 47–57, https://doi.org/10.1016/j.neurobiolaging.2019.02.029.

[34] S.P. Yasuda, Y. Seki, S. Suzuki, Y. Ohshiba, X. Hou, K. Matsuoka, K. Wada, H. Shitara, Y. Miyasaka, Y. c Kikkawa, 753A>G genome editing of a Cdh23(ahl) allele delays age-related hearing loss and degeneration of cochlear hair cells in C57BL/6J mice, Hear. Res. 389 (2020), 107926, https://doi.org/10.1016/j.heares.2020.107926.

[35] J.Y. Jeng, A.J. Carlton, S.L. Johnson, S.D.M. Brown, M.C. Holley, M.R. Bowl, W. Marcotti, Biophysical and morphological changes in inner hair cells and their efferent innervation in the ageing mouse cochlea, J. Physiol. 599 (1) (2021) 269–287, https://doi.org/10.1113/JP280256.

[36] K.R. Henry, R.A. Chole, Genotypic differences in behavioral, physiological and anatomical expressions of age-related hearing loss in the laboratory mouse, Audiology: Off. Organ. Int. Soc. Audiol. 19 (5) (1980) 369–383, https://doi.org/10.3109/00206098009070071.

[37] H. Zhang, K. Davies, H.J. Forman, Oxidative stress response and Nrf2 signaling in aging, Free Radic. Biol. Med. 88 (Pt B) (2015) 314–336, https://doi.org/10.1016/j.freeradbiomed.2015.05.036.

[38] M. Hirose, T. Hayano, H. Shirai, H. Nakamura, M. Kikuchi, Isolation of anti-glutathione antibodies from a phage display library, Protein Eng. 11 (3) (1998) 243–248.

[39] J. Kulig, J.F. Willott, Frequency difference limens of C57BL/6 and DBA/2 mice: relationship to auditory neuronal response properties and hearing impairment, Hear. Res. 16 (2) (1984) 169–174, https://doi.org/10.1016/0378-5955(84)90006-6.

[40] A.R. Fetoni, F. Paciello, R. Rolesi, S.L. Eramo, C. Mancuso, D. Troiani, et al., Rosmarinic acid up-regulates the noise-activated Nrf2/HO-1 pathway and protects against noise-induced injury in rat cochlea, Free Radic. Biol. Med. 85 (2015) 269–281.

[41] A.R. Fetoni, V. Zorzi, F. Paciello, G. Ziraldo, C. Peres, M. Raspa, et al., Cx26 partial loss causes accelerated presbycusis by redox imbalance and dysregulation of Nfr2 pathway, Redox Biol. 19 (2018) 301–317.

[42] A. Ayala, M.F. Munoz, S. Arguelles, Lipid peroxidation: production, metabolism, and signaling mechanisms of malondialdehyde and 4-hydroxy-2-nonenal, Oxid. Med. Cell. Longev. 2014 (2014), 360438.

[43] A. Bennaars-Eiden, L. Higgins, A.V. Hertzel, R.J. Kapphahn, D.A. Ferrington, D. A. Bernlohr, Covalent modification of epithelial fatty acid-binding protein by 4-hydroxynonenal in vitro and in vivo. Evidence for a role in antioxidant biology, J. Biol. Chem. 277 (52) (2002) 50693–50702.

[44] H. Motohashi, M. Yamamoto, Nrf2-Keap1 defines a physiologically important stress response mechanism, Trends Mol. Med. 10 (11) (2004) 549–557, https://doi.org/10.1016/j.molmed.2004.09.003.

[45] Q. Ma, Role of nrf2 in oxidative stress and toxicity, Annu. Rev. Pharmacol. Toxicol. 53 (2013) 401–426, https://doi.org/10.1146/annurev-pharmtox-011112-140320.

[46] H.J. Forman, H. Zhang, A. Rinna, Glutathione: overview of its protective roles, measurement, and biosynthesis, Mol. Aspect. Med. 30 (1–2) (2009) 1–12, https://doi.org/10.1016/j.mam.2008.08.006.

[47] P.Z. Wu, J.T. Malley, V. de Gruttola, M.C. Liberman, Age-related hearing loss is dominated by damage to inner ear sensory cells, not the cellular battery that powers them, J. Neurosci. 40 (33) (2020) 6357–6366, https://doi.org/10.1523/JNEUROSCI.0937-20.2020.

[48] C.O. Dirain, M. Ng, B. Milne-Davies, J.K. Joseph, P.J. Antonelli, Evaluation of mitoquinone for protecting against amikacin-induced ototoxicity in Guinea pigs, Otol. Neurotol. 39 (1) (2018) 111–118, https://doi.org/10.1097/MAO.0000000000001638.

[49] Y.R. Kim, J.I. Baek, S.H. Kim, et al., Therapeutic potential of the mitochondria-targeted antioxidant MitoQ in mitochondrial-ROS induced sensorineural hearing loss caused by Idh2 deficiency, Redox Biol. 20 (2019) 544–555, https://doi.org/10.1016/j.redox.2018.11.013.

[50] A.D. Tate, P.J. Antonelli, K.R. Hannabass, C.O. Dirain, Mitochondria-Targeted antioxidant mitoquinone reduces cisplatin-induced ototoxicity in Guinea pigs, Otolaryngol. Head Neck Surg. 156 (3) (2017) 543–548, https://doi.org/10.1177/0194599816678381.

[51] X. Qiu, K. Brown, M.D. Hirschey, E. Verdin, D. Chen, Calorie restriction reduces oxidative stress by SIRT3-mediated SOD2 activation, Cell Metabol. 12 (6) (2010) 662–667, https://doi.org/10.1016/j.cmet.2010.11.015.

[52] J.C. Jiang, E. Jaruga, M.V. Repnevskaya, S.M. Jazwinski, An intervention resembling caloric restriction prolongs life span and retards aging in yeast, Faseb. J. 14 (14) (2000) 2135–2137, https://doi.org/10.1096/fj.00-0242fje.

[53] S.J. Lin, P.A. Defossez, L. Guarente, Requirement of NAD and SIR2 for life-span extension by calorie restriction in Saccharomyces cerevisiae, Science 289 (5487) (2000) 2126–2128, https://doi.org/10.1126/science.289.5487.2126.
[54] E.J. Lesnefsky, C.L. Hoppel, Oxidative phosphorylation and aging, Ageing Res. Rev. 5 (4) (2006) 402–433, https://doi.org/10.1016/j.arr.2006.04.001.
[55] H. Takahashi, K. Jojiki, Water isotope effect on the lipidic cubic phase: heavy water-Induced interfacial area reduction of monoolein-Water system, Chem. Phys. Lipids 208 (2017) 52–57, https://doi.org/10.1016/j.chemphyslip.2017.09.001.
[56] C.L. Green, Q.A. Soltow, S.E. Mitchell, D. Derous, Y. Wang, L. Chen, J.J. Han, D.E. L. Promislow, D. Lusseau, A. Douglas, D.P. Jones, J.R. Speakman, The effects of graded levels of calorie restriction: XIII. Global metabolomics screen reveals graded changes in circulating amino acids, vitamins, and bile acids in the plasma of C57bl/6 mice, J. Gerontol. Series A, Biol. Sci. Med. Sci. 74 (1) (2019) 16–26, https://doi.org/10.1093/gerona/gly058.
[57] J.A. Gwin, D.D. Church, R.R. Wolfe, A.A. Ferrando, S.M. Pasiakos, Muscle protein synthesis and whole-body protein turnover responses to ingesting essential amino acids, intact protein, and protein-containing mixed meals with considerations for energy deficit, Nutrients 12 (8) (2020), https://doi.org/10.3390/nu12082457.
[58] M. Holecek, Branched-chain amino acids in health and disease: metabolism, alterations in blood plasma, and as supplements, Nutr. Metabol. 15 (2018) 33, https://doi.org/10.1186/s12986-018-0271-1.
[59] M. Iwasa, Y. Kobayashi, R. Mifuji-Moroka, N. Hara, H. Miyachi, R. Sugimoto, H. Tanaka, N. Fujita, E.C. Gabazza, Y. Takei, Branched-chain amino acid supplementation reduces oxidative stress and prolongs survival in rats with advanced liver cirrhosis, PLoS One 8 (7) (2013), e70309, https://doi.org/10.1371/journal.pone.0070309.
[60] V.M. Boer, C.A. Crutchfield, P.H. Bradley, D. Botstein, J.D. Rabinowitz, Growth-limiting intracellular metabolites in yeast growing under diverse nutrient limitations, Mol. Biol. Cell 21 (1) (2010) 198–211, https://doi.org/10.1091/mbc.E09-07-0597.
[61] J. Yuan, W.U. Fowler, E. Kimball, W. Lu, J.D. Rabinowitz, Kinetic flux profiling of nitrogen assimilation in Escherichia coli, Nat. Chem. Biol. 2 (10) (2006) 529–530, https://doi.org/10.1038/nchembio816.
[62] S.C. Hammel, K. East, A.J. Shaka, M.R. Rose, P. Shahrestani, Brief early-life non-specific incorporation of deuterium extends mean life span in Drosophila melanogaster without affecting fecundity, Rejuvenation Res. 16 (2) (2013) 98–104, https://doi.org/10.1089/rej.2012.1368.
[63] Z. Gyöngyi, F. Budán, I. Szabó, et al., Deuterium depleted water effects on survival of lung cancer patients and expression of Kras, Bcl2, and Myc genes in mouse lung, Nutr. Cancer 65 (2) (2013) 240–246, https://doi.org/10.1080/01635581.2013.756533.
[64] J. Berbée, I.M. Mol, G.L. Milne, et al., Deuterium-reinforced polyunsaturated fatty acids protect against atherosclerosis by lowering lipid peroxidation and hypercholesterolemia, Atherosclerosis 264 (2017) 100–107, https://doi.org/10.1016/j.atherosclerosis.2017.06.916.
[65] S. Vasdev, V. Prabhakaran, C.A. Sampson, Deuterium oxide normalizes blood pressure and vascular calcium uptake in Dahl salt-sensitive hypertensive rats, Hypertension 15 (2) (1990) 183–189, https://doi.org/10.1161/01.hyp.15.2.183.
[66] E. Charidemou, T. Ashmore, J.L. Griffin, The use of stable isotopes in the study of human pathophysiology, Int. J. Biochem. Cell Biol. 93 (2017) 102–109.